Electroluminescence of Multicomponent Conjugated Polymers. 2. Photophysics and Enhancement of Electroluminescence from Blends of Polyquinolines

Xuejun Zhang,[†] David M. Kale,[†] and Samson A. Jenekhe*[,‡]

Department of Chemical Engineering, University of Washington, Box 351750, Seattle, Washington 98195-1750, and Department of Chemical Engineering, University of Rochester, Rochester, New York 14627

Received July 12, 2001; Revised Manuscript Received October 17, 2001

ABSTRACT: Large enhancement in electroluminescence efficiency and brightness of light-emitting diodes fabricated from binary blends of conjugated polyquinolines was observed compared to devices made from the homopolymers. Blends of poly(2,2′-(2,5-thienylene)-6,6′-bis(4-phenylquinoline)) (PTPQ) and poly(2,2′-(biphenylene)-6,6′-bis(4-phenylquinoline)) (PBPQ), for example, had EL efficiency and luminance of up to a factor of 30 enhancement. Energy transfer was negligible in all four binary blend systems investigated. The electrical properties of the diodes and electric-field-modulated photoluminescence spectroscopy results confirmed that the enhancement of electroluminescence in the blends originated from spatial confinement of excitons which leads to increased exciton stability and electron−hole recombination efficiency. Voltage-tunable and composition-tunable multicolor electroluminescence was observed in the polymer blend devices. The observed composition-dependent new emission bands and enhanced fluorescence lifetimes in the blends were suggested to originate from exciplex formation and molecular miscibility between the blend components. These results demonstrate new phenomena in the electroluminescence and photophysics of multicomponent conjugated polymers.

Introduction

Blending of two or more polymers is a well-established strategy in polymer science and technology for manipulating the physical properties and performance of polymeric materials without the need to synthesize new polymers.[1] π-Conjugated polymers are molecular semiconductors with important electronic, optoelectronic, and photonic properties which are currently being exploited in various device applications. As such, blends of conjugated polymers are expected to be *supramolecular materials* or *alloys* in which novel properties and phenomena not found in the homopolymers can emerge as a result of synergistic *intermolecular interactions* between components of the mixture, *spatial confinement effects*, and *self-organization*. In principle, blends of conjugated polymers are thus very promising for the development of optimal materials for electronic, optoelectronic, and photonic applications.

Recent studies of blends of conjugated polymers have indeed shown them to exhibit novel supramolecular electronic, optoelectronic, and photonic properties such as optical absorption modulation,[2] photoinduced charge transfer,[2,3] bipolar conductivity,[4] enhanced photoconductivity,[3,5] efficient energy transfer,[6] enhanced electroluminescence,[7] and enhanced nonlinear optical properties.[8] Construction of organic quantum-well nanostructures, such as quantum wires and quantum boxes, by self-organization of blends of a block conjugated copolymer with a parent conjugated homopolymer[9] and facilitation of stimulated emission[10] and low-threshold amplified spontaneous emission[11] in blends of conjugated polymers have also been demonstrated.

Electroluminescence (EL) from blends of conjugated polymers has been described in several recent reports.[7,12] Voltage-tunable electroluminescence color was observed in phase-separated blends of several polythiophene derivatives having different emission colors.[12a] Phase separation of the blends on the 50−200 nm scale, which is comparable to or larger than the emitter thickness in the devices, was essential to the multicolor LED emission.[12a] White light EL emission has been observed from ternary blends of poly(3-(4-octylphenyl)-2,2′-bithiophene), poly(3-methyl-4-octylthiophene), and poly(3-cyclohexylthiophene),[13a] from binary blends of poly(2-methoxy-5-(2′-ethylhexoxy)-1,4-phenylenevinylene)) (MEH-PPV) with an alkoxy(trifluoromethyl)-stilbene-substituted poly(methyl acrylate) derivative (CF_3-PMA),[12c] from blends of a ladder-type poly(*p*-phenylene) (*m*-LPPP) with poly(perylene-*co*-diethylbenzene) (PPDB),[13b] and from ternary blends of polyquinolines. Enhancement in EL quantum efficiency and luminance of LEDs made from blends, compared to the component polymers, has been reported. Blends of poly(3-hexylthiophene) (P3HT) and MEH-PPV,[7b] blends of MEH-PPV, and a conjugated−nonconjugated multiblock copolymer (CNMBC), poly(1,3-propanedioxy-1,4-phenylene-1,2-ethylene(2,5-bis(trimethylsilyl)-1,4-phenylene)-1,2-ethenylene-1,4-phenylene),[7c] were reported to have enhanced EL efficiency. The mechanism of the observed EL enhancement was attributed to Forster-type energy transfer from MEH-PPV to P3HT or from CNMBC to MEH-PPV.[7b,c]

In addition to excitation energy transfer, several other processes or mechanisms are possible in the photophysics and EL of polymer blends depending on the electronic structures of the component conjugated polymers. Ground-state charge transfer or complex formation,[4] excited-state complex (exciplex) formation,[14] photoinduced electron transfer,[2,3] and exciton confinement[9b] are possible. However, depending on the relative lowest unoccupied molecular orbital (LUMO) and highest oc-

[†] University of Rochester.
[‡] University of Washington.

10.1021/ma0112164 CCC: $22.00
Published on Web 12/11/2001

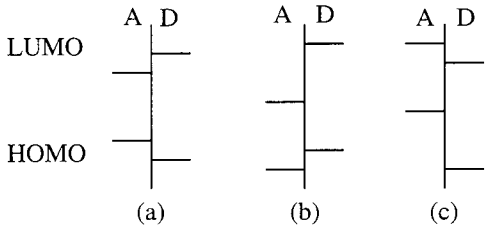

Figure 1. Schematic illustration of some possible relative energy levels of polymers A and D in a binary polymer blend A:D ($E_g^D > E_g^A$).

cupied molecular orbital (HOMO) levels of polymers A and D (here we assume that the HOMO−LUMO gaps are such that $E_g^D > E_g^A$) in a blend (denoted A:D), the dominant process may be different in the three cases of HOMO/LUMO level pairs illustrated in Figure 1. These diverse photophysical and charge-transfer processes are yet to be fully delineated and understood in blends of electroluminescent conjugated polymers. In a previous paper, we investigated the roles of polymer/polymer interfaces in the electroluminescence of multicomponent conjugated polymer systems by using bilayer thin films.[15a]

In this paper, we report the electroluminescence and photophysics of several binary blends of conjugated polyquinolines. In particular, we used these blends as model systems to explore the roles of the electronic structure of the component polymers, excitation energy transfer, exciplex formation, spatial confinement of excitons, and morphology on the EL efficiency and features of LEDs fabricated from multicomponent conjugated polymer systems. The polyquinolines used in this study include poly(2,6-(4-(*p*-*tert*-butyl)phenylquinoline)) (Bu-PQ), poly(2,2′-(*p*-phenyl)-6,6′-bis(4-(*p*-*tert*-butyl)phenylquinoline)) (Bu-PPQ), poly(2,2′-(biphenylene)-6,6′-bis(4-phenylquinoline)) (PBPQ), poly(2,2′-(*p*-phenyl)-6,6′-bis(4-phenylquinoline)) (PPPQ), and poly(2,2′-(2,5-thienylene)-6,6′-bis(4-phenylquinoline)) (PTPQ). Molecular structures of these conjugated polyquinolines are shown in Chart 1 along with other materials. Four binary blend systems, PTPQ:PBPQ, Bu-PQ:PBPQ, Bu-PQ:Bu-PPQ, and PPPQ:Bu-PPQ, were prepared and investigated by steady-state photoluminescence, picosecond time-resolved fluorescence decay measurements, and electric-field-modulated photoluminescence spectroscopy. The EL spectra and performance of LEDs made from these blends were investigated as a function of blend composition.

Experimental Section

Materials. All the polyquinolines used in this study were previously synthesized in our laboratory.[16] The synthesis, characterization, thin film processing, optical and nonlinear optical properties, electrochemistry, photoconductivity, and electroluminescence of these and many other polyquinolines were previously reported by our group.[15,16] The polyquinolines used in this study had intrinsic viscosities of 3−12 dL/g, which were measured in 0.1 mol % di-*m*-cresyl-phosphate/*m*-cresol at 25 °C or in methanesulfonic acid at 30 °C, indicating that they are high molecular weight polymeric materials. Since all the polyquinolines are good electron transport (n-type) and emissive materials, their electroluminescence was investigated in a bilayer device structure including a hole transport layer consisting of 1,1-bis(di-4-tolylaminophenyl)cyclohexane (TAPC) dispersed in polystyrene (PS).[17a] TAPC was provided by Eastman Kodak Co. (Rochester, NY). PS with a molecular weight (M_n) of ∼200 000 was obtained from Polysciences. The molecular structures of the materials used in this study are shown in Chart 1.

Chart 1

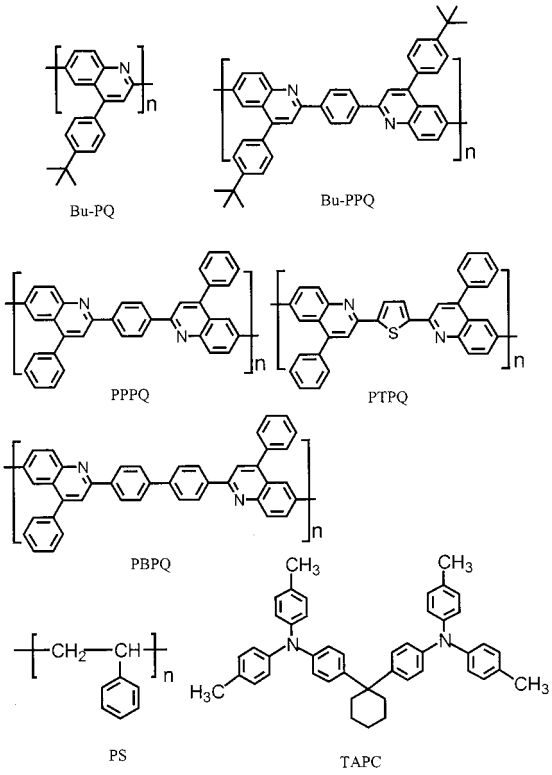

Preparation of Blends and Thin Films. Binary blends of polyquinolines were prepared by dissolving the binary mixtures in formic acid in which both polymers are very soluble. The resulting solutions (0.3−0.4 wt % total polymers) were homogeneous. Compositions of blends (A:D) in this paper refer to weight percentage of polymer A. Four series of blend compositions were prepared in this study. For example, 0.1, 1, 5, 10, 20, 30, and 50 wt % PTPQ:PBPQ blends were prepared. Since PTPQ and PBPQ have close repeat unit molecular weights (488.6 for PTPQ and 558.7 for PBPQ), the concentrations of PTPQ in wt % and in mol % are close.

Although prior studies of blends of various conjugated polymers[2,4,6] in our group have used complexation mediated processing,[17b,c] all thin films of the homopolymers or blends reported here were obtained by spin-coating from formic acid solutions. Films for optical absorption and photoluminescence measurements were spin-coated onto silica substrates. All the films were dried overnight at 60 °C in a vacuum to remove any residual solvent. Blend films (25−35 nm thick) were homogeneous and showed excellent optical transparency. No visible phase separation was observed. The good miscibility between polyquinolines is due to their structural similarities. Because of a lack of contrast, attempts to use transmission electron microscopy (TEM) to probe the morphology of these polyquinoline blends were not successful. Since PBPQ and PTPQ emit orange and red color, respectively, we also applied an Olympus BX60 fluorescence microscope (Olympus America, Melville, NY) to investigate the morphology of blends. No features were resolved, indicating homogeneity and good miscibility in blends or that the phase separation domains, if any, are less than the resolution of the fluorescence microscope (∼500 nm). Miscibility on a much smaller scale was subsequently indicated from photoluminescence and electroluminescence studies of the blends.

Optical Absorption and Photoluminescence Spectroscopy. Optical absorption spectra were obtained by using a Lambda-9 UV/vis/near-IR spectrophotometer (Perkin-Elmer). Steady-state photoluminescence (PL) studies were carried out on a Spex Fluolog-2 spectrofluorimeter. The films were positioned such that the emitted light was detected at 22.5° from the incident beam. The relative PL quantum efficiencies of blends and homopolymers were determined from the inte-

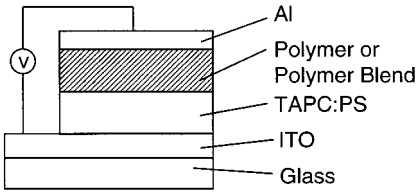

Figure 2. Schematic structure of polymer blend LED.

grated intensity of the PL spectra which were corrected for absorbance at the excitation wavelength.[18]

Time-Resolved Photoluminescence Decay Dynamics. Picosecond time-resolved photoluminescence decay measurements were performed by using the time-correlated single photon counting technique.[18] The excitation system consists of a cavity pumped dye laser (Coherent model 703D) circulating rhodamine 6G, synchronously pumped by a mode-locked frequency-doubled Nd:YAG laser (Quantronics model 416). The dye laser pulses were typically 10 ps duration at a repetition rate of 38 MHz, and the samples were excited at 380 nm. The PL decay was detected at the emission peak wavelength.

Fabrication and Characterization of LEDs. Electroluminescent devices were fabricated and investigated as sandwich structures between aluminum (Al) and indium−tin oxide (ITO) electrodes (Figure 2). 1,1-Bis(di-4-tolylaminophenyl)-cyclohexane (TAPC) dispersed in polystyrene (PS) was used as the hole-transport layer (HTL).[17a] The TAPC:PS (50 wt %) thin films (50 nm) were deposited onto ITO-coated glass substrates (Donelly Corp., Holland, MI) by spin-coating from dichloromethane solutions. Thin films (25−40 nm) of conjugated polyquinolines or their blends were spin-coated from their formic acid solution onto the TAPC:PS layer and dried at 60 °C in a vacuum overnight. The film thicknesses were measured by an Alpha-step profilometer (Tencor Northern, San Jose, CA) with an accuracy of ±1 nm and confirmed by an optical absorption coefficient technique. Finally, 100−130 nm aluminum electrodes were vacuum (5×10^{-6} Torr) evaporated onto the resulting bilayers. The area of each EL device was 0.2 cm^2. Electroluminescence spectra were obtained by using a Spex Fluorolog-2 spectrofluorimeter. Current−voltage ($I-V$) and luminance−voltage ($L-V$) curves were recorded simultaneously by hooking up an HP4155A semiconductor parameter analyzer (Yokogawa Hewlett-Packard, Tokyo) together with a Grasby S370 optometer (Grasby Optronics, Orlando) equipped with a model 211 luminance sensor head. The EL quantum efficiencies of the diodes were estimated by using procedures similar to that previously reported.[15a,b] All the fabrication and measurements were done under ambient laboratory conditions.

Electric-Field-Modulated Photoluminescence Spectroscopy. Electric-field-modulated PL measurements were performed on the same electroluminescent devices described above after their EL properties have been characterized. An LED sample is photoexcited, and the PL emission spectrum is acquired under an applied bias voltage. Both forward (positive to ITO) and reverse bias voltages gave identical PL spectra before EL emission. The device was positioned such that the emitted light was detected from the ITO side at 22.5° relative to the incident beam. All the experimental conditions are the same as in steady-state PL measurements of thin films on silica substrates.

Results and Discussion

Electronic Structures of Polyquinolines. Figure 3a shows the optical absorption spectra of polyquinoline thin films. The absorption maxima and the optical band gaps determined from the absorption edges are listed in Table 1. The onset reduction and oxidation potentials measured from cyclic voltammetry are also listed in Table 1. Bu-PPQ, PPPQ, and PBPQ have very close absorption peaks and band gaps due to their structural similarities. However, Bu-PQ and PTPQ show bathochromic shifts in both the absorption peaks and band gaps. For example, Bu-PPQ and PPPQ have absorption peaks at 399 and 400 nm, respectively, and the same

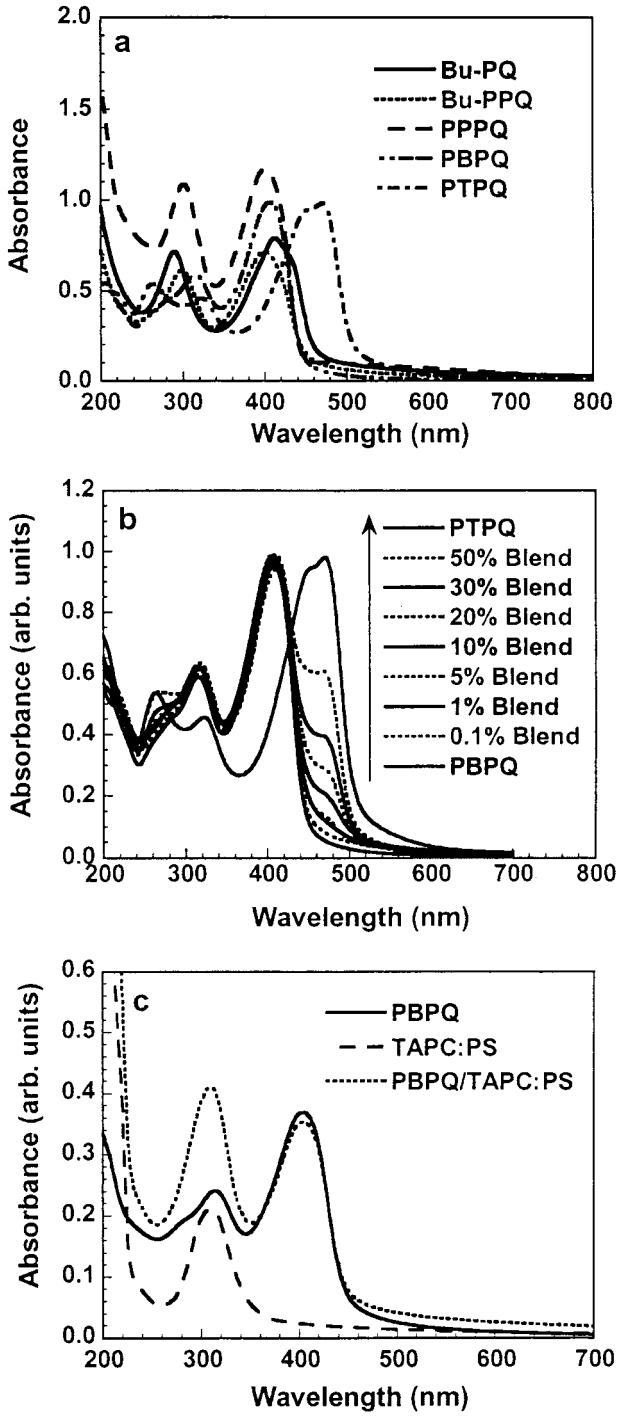

Figure 3. Optical absorption spectra of thin films on silica substrates: (a) polyquinoline homopolymers; (b) PTPQ, PBPQ, and their blends; (c) PBPQ, TAPC:PS, and PBPQ/TAPC:PS.

Table 1. Optical and Electronic Properties of Polyquinolines

polymer	λ_{max}^{ABS}, nm	λ_{max}^{PL}, nm	E_g^{opt}, eV	E_{red},[a] V	E_{ox},[b] V
Bu-PQ	412	574	2.65	−1.86	0.79
Bu-PPQ	399	540	2.78	−1.58	1.20
PPPQ	400	571	2.78	−1.90	0.88
PBPQ	405	571	2.81	−1.98	0.83
PTPQ	471	622	2.49	−1.84	0.65

[a] E_{red} values are onset potentials vs SCE. The data are from refs 7d and 16a. [b] E_{ox} was calculated from $E_{ox} = E_g^{opt} - |E_{red}|$.

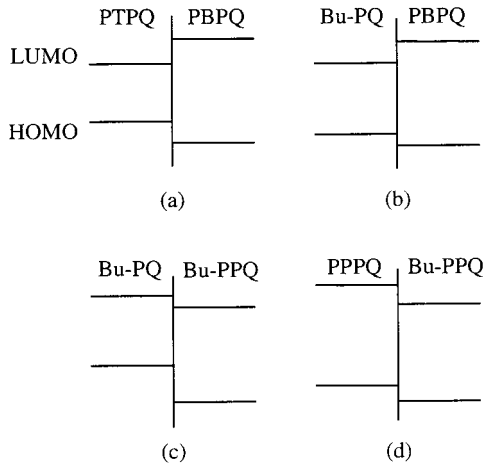

Figure 4. Schematic of the HOMO−LUMO levels of the four polyquinoline blend systems investigated.

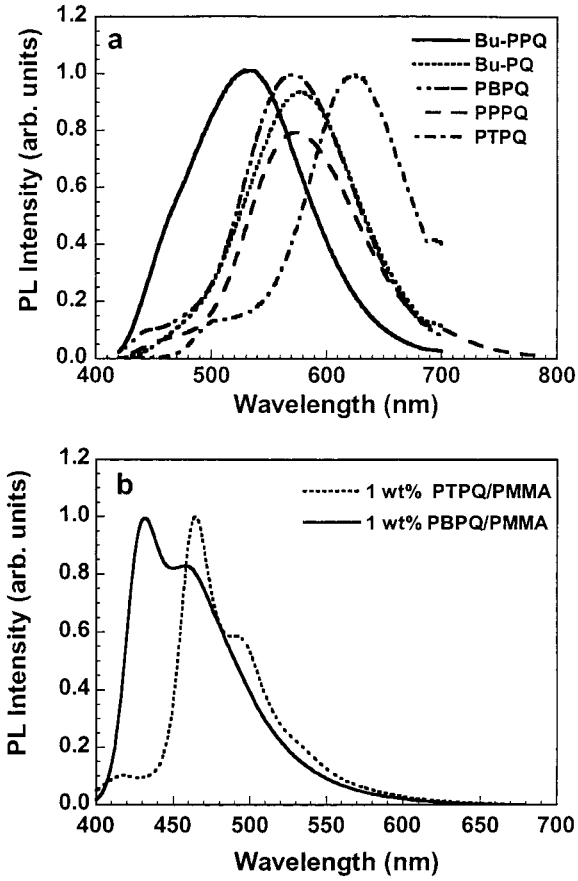

Figure 5. PL spectra of thin films: (a) polyquinoline homopolymers; (b) PTPQ and PBPQ dispersed in PMMA. The excitation wavelength was 400 nm for all spectra except those of PTPQ (430 nm).

band gap of 2.78 eV. PBPQ has an absorption peak at 405 nm and a band gap of 2.81 eV. Bu-PQ has an absorption peak at 412 nm and a band gap of 2.65 eV. PTPQ has an absorption peak at 471 nm and a band gap of 2.49 eV. The relative HOMO and LUMO levels of these polyquinolines can be represented by their oxidation and reduction potentials. Figure 4 schematically illustrates the HOMO−LUMO levels of the four blends investigated in this study. PTPQ:PBPQ and Bu-PQ:PBPQ blends are very similar. The PPPQ:Bu-PPQ blend system is similar to Bu-PQ:Bu-PPQ except that PPPQ and Bu-PPQ have the

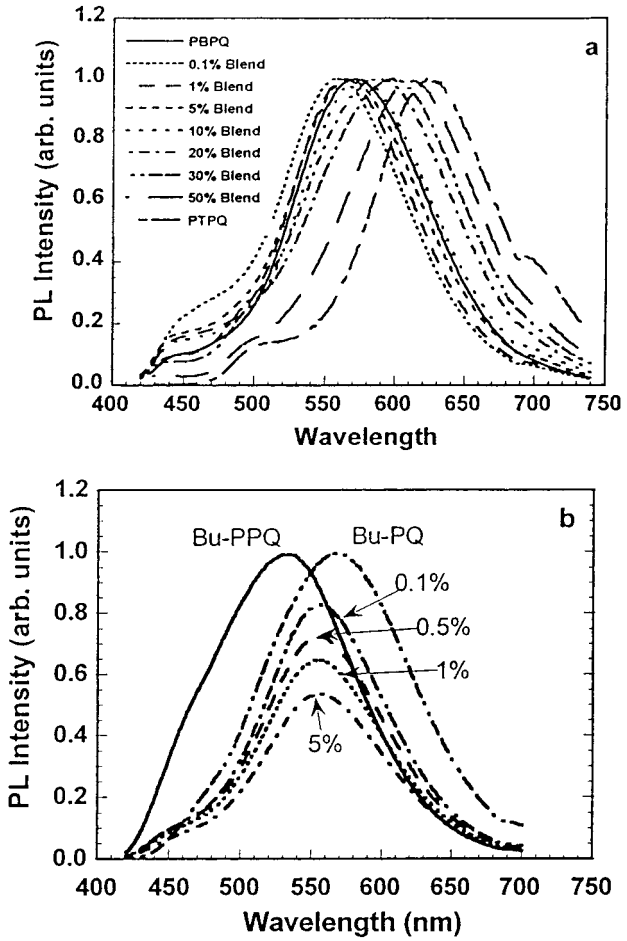

Figure 6. PL spectra of thin films: (a) PTPQ, PBPQ, and their blends; (b) Bu-PQ, Bu-PPQ, and their blends. All blends and PBPQ were excited at 400 nm, and PTPQ was excited at 430 nm.

same band gaps. These relative HOMO−LUMO levels of the homopolymers are important in rationalizing the photophysical and charge transport/trapping processes in the binary blends.

Optical Absorption Spectra. The optical absorption spectra of thin films of PTPQ, PBPQ, and their blends are shown in Figure 3b. PBPQ has an absorption peak at 405 nm and an absorption band edge around 441 nm (2.81 eV). PTPQ has an absorption peak at 475 nm and an absorption band edge around 506 nm (2.49 eV). The absorption spectra of the blends are almost identical to that of PBPQ at low concentrations (0.1−1%) of PTPQ. However, at higher concentrations (5−50%) of PTPQ, the absorption band of PTPQ clearly shows up as a lower energy shoulder in the absorption spectra of the blends. The absorption spectra of the binary blends are simple superposition of those of PBPQ and PTPQ. New absorption features were not observed in the wavelength range of 200−2800 nm, suggesting that the two blend components have no observable interactions in their electronic ground states. Similar results were observed in Bu-PQ:PBPQ, Bu-PQ:Bu-PPQ, and PPPQ:Bu-PPQ blends.

The optical absorption spectra of bilayer films of the blends or homopolymers with the hole-transport layer TAPC:PS used in LED devices were also measured. Figure 3c shows such a representative spectrum of PBPQ/TAPC:PS bilayer along with those of the PBPQ and TAPC:PS single layers. The spectrum of the PBPQ/

Table 2. PL and EL Data for PTPQ:PBPQ Blend System

wt % PTPQ	λ_{max}^{PL}, nm	rel PL efficiency	film thickness in EL device, nm	turn-on voltage, V	EL peak, nm (voltage, V)
0.0	571	0.86	30	7.0	557 (8)
0.1	559	1.00	30	7.0	542 (8)
1.0	562	0.66	30	7.0	504 (8)
5.0	567	0.49	25	7.0	551 (8)
10.0	574	0.40	30	7.5	581 (8)
20.0	586	0.46	35	6.0	554 (8)
30.0	596	0.40	30	5.5	560 (8)
50.0	608	0.36	35	6.0	556 (8)
100.0	622	0.17	40	4.5	622 (5)

TAPC:PS bilayer is a simple superposition of those of PBPQ and TAPC:PS single layers, indicating that there is no complex formation between PBPQ and TAPC in their ground states. Similar results were found for bilayers of other polyquinolines or blends with TAPC:PS.

Photoluminescence. PL spectra of thin films of the polyquinolines investigated are shown in Figure 5a. The PL emission peaks of the polyquinolines are listed in Table 1. The PL emission colors of these polyquinolines are green-yellow (Bu-PPQ), orange (Bu-PQ, PPPQ, and PBPQ), and red (PTPQ). These polymers showed structureless PL emission spectra with a large Stokes shift ranging from 139 nm for Bu-PPQ to 171 nm for PPPQ. The broad, featureless PL emission spectra and the large Stokes shifts of these polyquinolines are characteristic of intermolecular excimer emission which has previously been observed in many conjugated polymers[14a] and self-organized block copolymers containing polyquinolines.[19] However, the single-chain emission of even excimer-forming conjugated polymers can usually be observed in dilute fluid or solid solutions.[14a] Figure 5b shows the PL emission spectra of PBPQ and PTPQ in an inert poly(methyl methacrylate) (PMMA) solid matrix (1 wt %). The PL emission spectrum of PBPQ in PMMA has a peak at 432 nm and a shoulder around 450 nm. The PL emission spectrum of the 1 wt % PTPQ:PMMA, on the other hand, has a peak at 464 nm and a shoulder around 500 nm. These more structured PL spectra of PBPQ and PTPQ exhibit very small Stokes shifts and can be assigned to the single-chain emission (singlet intrachain excitons) of the polymers.[14a]

The PL spectra of PTPQ, PBPQ, and their blends are shown in Figure 6a. The spectrum of PTPQ (430 nm excitation) has an emission peak at 622 nm and a minor emission band around 500 nm. In contrast, the PL spectrum of PBPQ (400 nm excitation) has a peak at 571 nm and a minor band at 450 nm. Comparison of the PL spectra (Figure 5a) with optical absorption spectra (Figure 3a) of these polyquinolines shows that there is little spectral overlap between the absorption of PTPQ and the emission of PBPQ. Therefore, energy transfer from the excited PBPQ to PTPQ is negligible in these blends. On the same grounds, energy transfer can also be ruled out in the Bu-PQ:PBPQ, Bu-PQ:Bu-PPQ, and PPPQ:Bu-PPQ blends. Unlike previously reported blends of EL polymers, in which energy transfer was significant,[7b,c] our blend systems show negligible energy transfer. Therefore, other photophysical mechanisms that may affect the electroluminescence of polymer blends such as exciplex formation and spatial confinement of excitons can be more easily explored.

The normalized PL spectra of thin films of PTPQ:PBPQ blends are shown in Figure 6a. Either a slight blue shift (0.1−5% PTPQ) or a red shift (10−50% PTPQ) in emission peaks, relative to the PL spectrum of PBPQ, is observed depending on the blend composition. The emission peaks of the blends are listed in Table 2. It was also found that the blue emission band around 450 nm in the blends of low PTPQ concentrations (0.1−5%) was enhanced compared to that in pure PBPQ. This blue emission band is at the same location as the single-chain emission of PTPQ in a matrix of PMMA as evidenced in Figure 5b. However, whereas PMMA is an inert matrix, PBPQ is an electroactive and photoactive conjugated polymer ("host chromophore") that can interact with the "guest chromophore" (PTPQ) in the excited state. Therefore, a careful consideration is essential to interpret the blend PL spectra. Excimer emission is known to be dominant in the PL of thin films of many conjugated polymers,[14a] including the polyquinolines.[15] In binary blends (A:D) of conjugated homopolymers A and D, both single-chain (A*, D*) and excimer ((AA*), (DD*)) emission can thus be expected, depending on the scale of miscibility. In addition, exciplex ((A*D) or (AD*)) can also occur in the blends. Because the observed PL spectra of the blends are very distinct and are not superpositions of those of the component polymers, exciplex formation between PTPQ and PBPQ appears to be the simplest explanation. However, the presence of a higher energy component in the 440−510 nm region indicates that single-chain emission is also present in the PL spectra.

Table 3. PL and EL Data for Bu-PQ:PBPQ, Bu-PQ:Bu-PPQ, and PPPQ:Bu-PPQ Blends

blends (A:D)	composn, wt % A	PL peak, nm	rel PL efficiency	film thickness for EL device, nm	turn-on voltage, V	EL peak, nm
Bu-PQ:PBPQ	0	574	0.45	60	9	557
	0.1	556	0.51	55	8	567
	0.5	561	0.55	55	9	562
	1.0	567	0.62	55	9	558
	100	571	1.0	30	7	586
Bu-PQ:Bu-PPQ	0	540	1.53	50	8	539
	0.1	556	1.44	60	9	531
	0.5	554	1.27	65	10	539
	1.0	554	1.16	60	9	542
	5.0	558	0.99	65	10	539
	100	574	1.0	60	9	586
PPPQ:Bu-PPQ	0	540	3.10	50	8	539
	0.1	538	3.13	55	9	546
	0.5	539	3.11	50	8	542
	1.0	541	3.16	50	8	547
	5.0	546	2.98	50	8	542
	100	571	1.0	50	9	580

We can also infer molecular level miscibility of these binary blends from the new emission spectra since any nanoscale (or higher level) phase separation would have resulted in blend PL spectra composed of the component homopolymer spectra. Figure 6b shows representative PL spectra of the Bu-PQ:Bu-PPQ blend system. The PL spectra for Bu-PQ:PBPQ, Bu-PQ:Bu-PPQ, and PPPQ:Bu-PPQ blends are summarized in Table 3. The PL spectra of all the blends were found to depend on composition as seen in Figure 6 and Tables 2 and 3. These latter blend PL spectra originate from the same excited states as discussed above for the PTPQ:PBPQ blend system, i.e., mostly exciplex emission with a blue component due to single-chain excitons.

The relative PL quantum efficiencies shown in Table 2 were estimated by comparing the integrated PL spectra taken under the same experimental conditions and corrected by the absorbance at the excitation wavelength. The results show that the 0.1% and 1% blends have quantum efficiencies that are very close to the pure PBPQ, but the quantum efficiency of PTPQ is about 5 times lower than that of PBPQ. The relative PL efficiencies of the blends decrease with increasing amount of PTPQ. The absence of enhancement of the PL quantum efficiency in these blends further confirms the absence of excitation energy transfer in the PTPQ:PBPQ blends.

The PL spectra of PTPQ, PBPQ, and their blends were also measured by using the LED samples (Figure 7). This was done to facilitate later comparisons between PL and EL spectra. The main concern is to clarify any possible interactions between the emissive polymers or blends and the hole-transport molecule TAPC in the excited state. In Figure 7a, the ITO/PTPQ and ITO/TAPC/PTPQ films showed identical PL spectra. However, the ITO/PBPQ and ITO/TAPC/PBPQ samples showed dramatically different PL spectra (Figure 7b). The ITO/TAPC/PBPQ bilayer film showed a broader and blue-shifted emission band compared to the ITO/PBPQ single-layer film. While the PBPQ emission band, with peak near 560−570 nm, is still present, an intense blue component in the 430−490 nm emerges in the bilayer. Similar results were found for the 0.1% blend as shown in Figure 7c. This observation of spectral changes in the presence of TAPC raises the question of whether exciplex formation between PBPQ and TAPC had occurred in the bilayer. Exciplex formation between several acceptor π-conjugated polymers and triarylamine molecules has been reported.[14a,b,18c] However, TAPC has an absorption edge of ~350 nm (Figure 3c), i.e., an optical band gap of ~3.5 eV. The oxidation potential of TAPC was reported to be 0.91 V vs saturated calomel electrode (SCE),[20] which is a little higher than the values for most polyquinolines (Table 1). Therefore, if the polyquinoline/TAPC bilayer film was excited at a wavelength above 350 nm, only Bu-PPQ/TAPC has the possibility of forming an exciplex. The PL spectrum of PBPQ/TAPC in Figure 7b was obtained with 400 nm excitation. Thus, we rule out PBPQ/TAPC exciplex emission as the origin of the observed spectral changes in the bilayers of Figure 7b,c. The emission of the PBPQ/TAPC bilayer is likely due to waveguide or microcavity effects. It is well-known that the microcavity structure in EL devices can greatly modify the emission spectrum of the device.[21] Since the PTPQ/TAPC or blend (>10%)/TAPC bilayers showed identical PL spectra as the corresponding single polymer layers, the observed spectral changes in PBPQ/TAPC or 0.1% blend/TAPC may be due to refractive index differences between PTPQ and PBPQ which may favor microcavity effects in PBPQ.

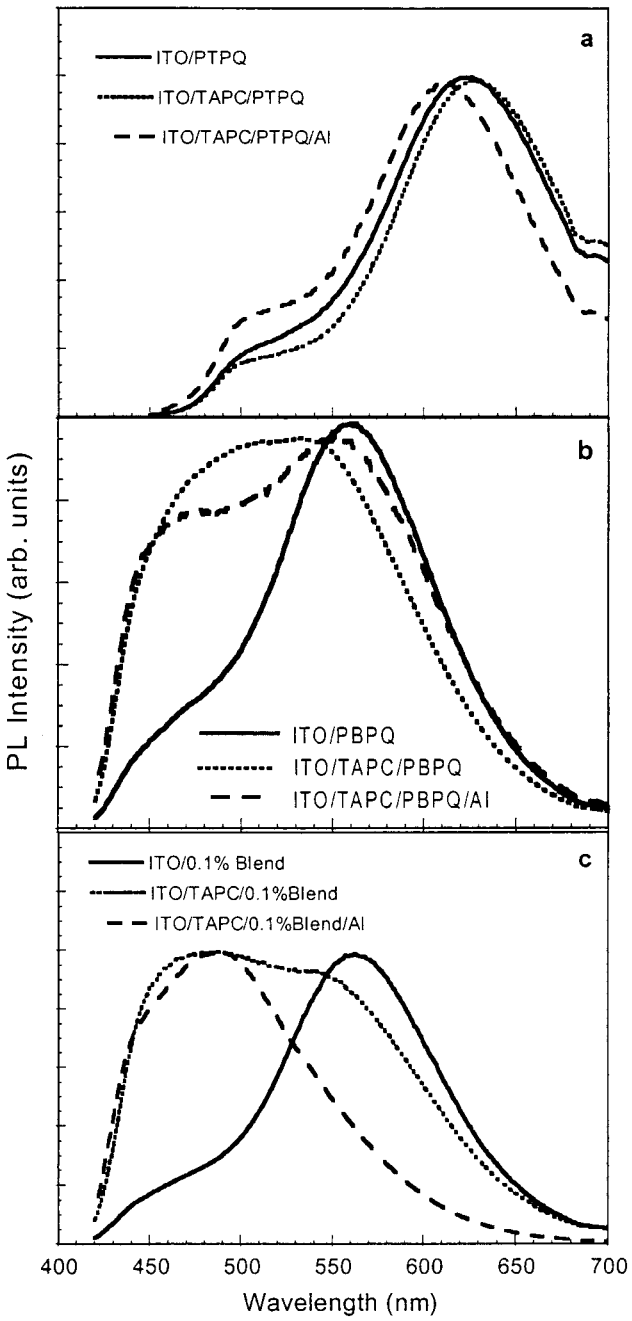

Figure 7. PL spectra of (a) ITO/PTPQ, ITO/TAPC/PTPQ, and ITO/TAPC/PTPQ/Al (excited at 430 nm); (b) ITO/PBPQ, ITO/TAPC/PBPQ, and ITO/TAPC/PBPQ/Al (excited at 400 nm); and (c) ITO/0.1% blend, ITO/TAPC/0.1% blend, and ITO/TAPC/0.1% blend/Al (excited at 400 nm).

Time-Resolved Photoluminescence Decay Dynamics. Representative picosecond time-resolved PL decay curves of PTPQ:PBPQ blends and the homopolymers are shown in Figure 8. The PL decay dynamics were best described by a three-term exponential function. The lifetimes and their amplitudes, obtained by the least-squares fitting of the PL decay data, are listed in Table 4. PTPQ has a shorter lifetime (1.99 ns) compared to PBPQ (2.45 ns). Similar to the steady-state PL spectra of Figure 6a, the PL decay dynamics of blends of these two polymers were highly composition dependent. The dilute blends (0.1−10% PTPQ) had longer lifetimes compared to that of either homopoly-

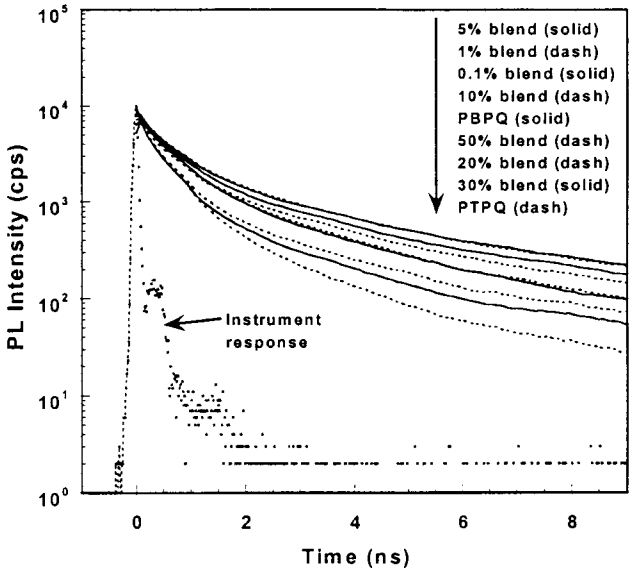

Figure 8. Time-resolved PL decay dynamics of PTPQ:PBPQ blends and homopolymers (380 nm excitation, emission was monitored at the PL peak).

Table 4. PL Decay Lifetimes of the PTPQ:PBPQ Blend System

wt % PTPQ	τ_1, ns	τ_2, ps	τ_3, ps	amplitude $\tau_1/\tau_2/\tau_3$
0	2.45	530	110	53/34/13
0.1	2.52	450	90	64/28/8
1	2.75	510	120	66/25/9
5	2.87	560	130	65/24/11
10	2.66	510	110	59/28/13
20	2.22	430	100	48/32/20
30	2.14	440	100	43/34/23
50	2.33	510	110	60/28/12
100	1.99	480	110	35/40/25

mer. The 20−50% blends had shorter lifetimes than PBPQ homopolymer. The observed composition-dependent PL decay dynamics of the blends can be understood to arise from changes in blend supramolecular structure or local morphology and is consistent with emission from PTPQ:PBPQ exciplexes.

Although transmission electron microscopy could not reveal any differences in morphology between the blends and homopolymers, a schematic illustration of the composition-dependent supramolecular structures of the blends is shown in Figure 9. At very low concentrations, single chains of PTPQ are completely surrounded by chains of PBPQ (Figure 9b). Since the HOMO−LUMO energy gap of PTPQ is smaller than that of PBPQ (Figure 4a), excitons generated in isolated PTPQ chains are effectively confined as single-chain excitons or as exciplexes with nearby PBPQ chains. In either case longer lifetimes as observed in the 0.1−10% blend can result. With increasing concentration of PTPQ in the blends (Figure 9c,d), multiple interactions and contacts between PTPQ and PBPQ chains arise, and this can weaken or eliminate exciton confinement in single chains or in exciplexes.

Electroluminescence. The EL spectra of polyquinolines and their blends at low bias voltages were found to be similar to the corresponding PL spectra. At higher forward bias voltages, EL spectra of blends were significantly blue-shifted from the corresponding PL spectra. Representative EL spectra of PTPQ, PBPQ, and some of their blends are shown in Figure 10. The EL spectrum of PTPQ in Figure 10b is identical to the PL

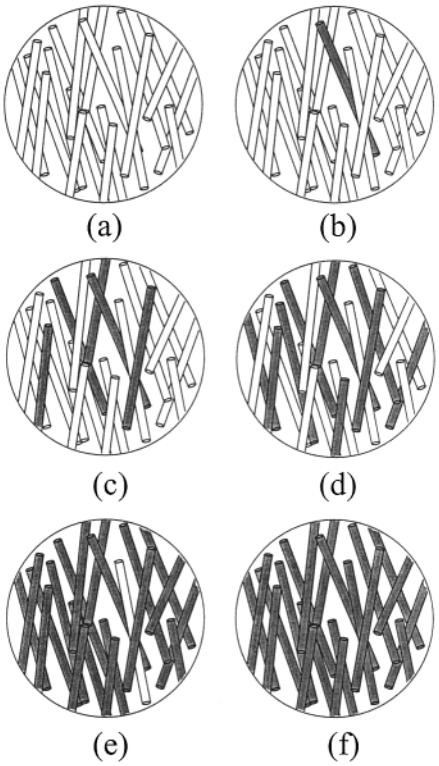

Figure 9. Schematic illustration of the local morphology of binary blends of conjugated polyquinolines: (a) and (f), homopolymers; (b), (c), (d), and (e), blends.

spectrum in Figure 5a, showing an emission peak at 622 nm. This suggests that the EL and PL emissions of this polymer originate from the same excited state. PBPQ showed an EL emission peak at 557 nm at a bias voltage of 8 V. The EL spectra of PTPQ:PBPQ blends (0.1, 5, 10, and 30%) are also shown in Figure 10. The EL emission peaks of the blends under a bias voltage of 8 V are listed in Table 2. It was found that the EL spectra of both PBPQ and the 0.1% blend varied with the bias voltage. In the case of PBPQ (Figure 10a), the EL emission peak shifted from 557 nm (yellow) at 8 V to 520 nm (green) at 13 V, and the EL intensity from the 450 nm blue band increased with increasing bias voltage.

The most striking EL blue shift with bias voltage was observed in the 0.1% blend (Figure 10c). The EL emission peak of the 0.1% blend was found to go from 547 nm (yellow) to 500 nm (blue-green) when the applied bias voltage was changed from 8 to 15 V. The 0.1% blend showed a much more dramatic increase in the EL intensity from the blue band with increasing voltage than PBPQ. For example, at 15 V, the EL intensity of the blue band (445 nm) is almost the same as that of the 500 nm band. The blue shift of the EL spectrum with increasing bias voltage was also observed in the 1−5% blends. Voltage tunability of the EL emission was negligible in the 10−50% blends. The enhanced EL emission in the blue band is due to the enhanced emission from higher energy states, such as the PTPQ single chains in which excitons are spatially confined. These blend EL spectra results are to be contrasted with those observed in binary blend systems exhibiting energy transfer where enhanced emission from the dispersed, minority, and lower-energy component is usually observed at the expense of the higher-energy matrix.[7b,c]

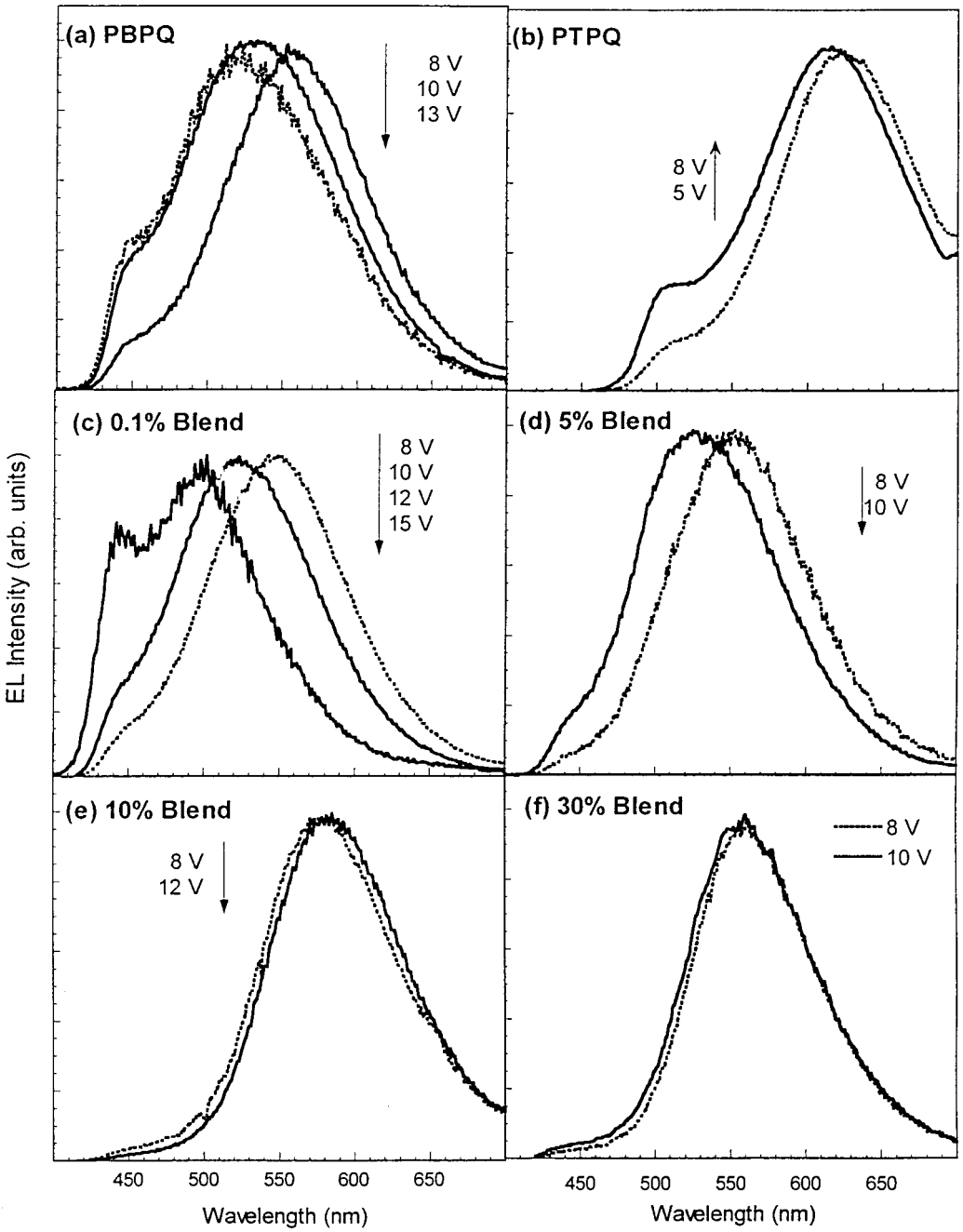

Figure 10. EL spectra of (a) PBPQ, (b) PTPQ, (c) 0.1% blend, (d) 5% blend, (e) 10% blend, and (f) 30% PTPQ:PBPQ blend system.

The EL spectra of the other three blend systems (Bu-PQ:Bu-PPQ, Bu-PQ:PBPQ, and PPPQ:Bu-PPQ) are shown in Figure 11. The composition dependence of the EL spectra was also observed. EL emission was clearly not from the lower energy component, again ruling out energy transfer in these binary blends.

The turn-on voltage characteristics of the blend LEDs, as determined by either current−voltage ($I-V$) or luminance−voltage ($L-V$) curves, were in the ranges of 6−7.5, 8−9, 9−10, and 8−9 V for the PTPQ:PBPQ, Bu-PQ:PBPQ, Bu-PQ:Bu-PPQ, and PPPQ:Bu-PPQ blend systems, respectively (Tables 2 and 3). These turn-on voltages are essentially identical to those of the corresponding homopolymer devices. All the LEDs turned on around 10^6 V/cm. Figure 12a shows current density−electric field characteristics for EL devices from PTPQ:PBPQ blends. All these devices have the same TAPC:PS hole-transport layer thickness of 50 nm; the emission layer thicknesses were in the 25−40 nm range and are listed in Table 2. The PTPQ device has the lowest turn-on voltage of ∼4.5 V (0.5 MV/cm), the PBPQ homopolymer devices and the 0.1−10% blends have almost the same turn-on voltage of 7−7.5 V (0.9−1 MV/cm), and the 20−50% blends showed turn-on voltages of 5.5−6 V. The turn-on voltage data for all devices are listed in Table 2. The lowest turn-on voltage observed for PTPQ devices is apparently because of its favorable HOMO/LUMO levels which give lower barriers for both electron and hole injections into the PTPQ layer compared to PBPQ. That the 0.1−10% blends have the same turn-on voltage as PBPQ indicates that electron and hole injections into the blends are controlled by the properties of the matrix polymer PBPQ. Figure 12a also shows that blend LEDs have a lower current than the

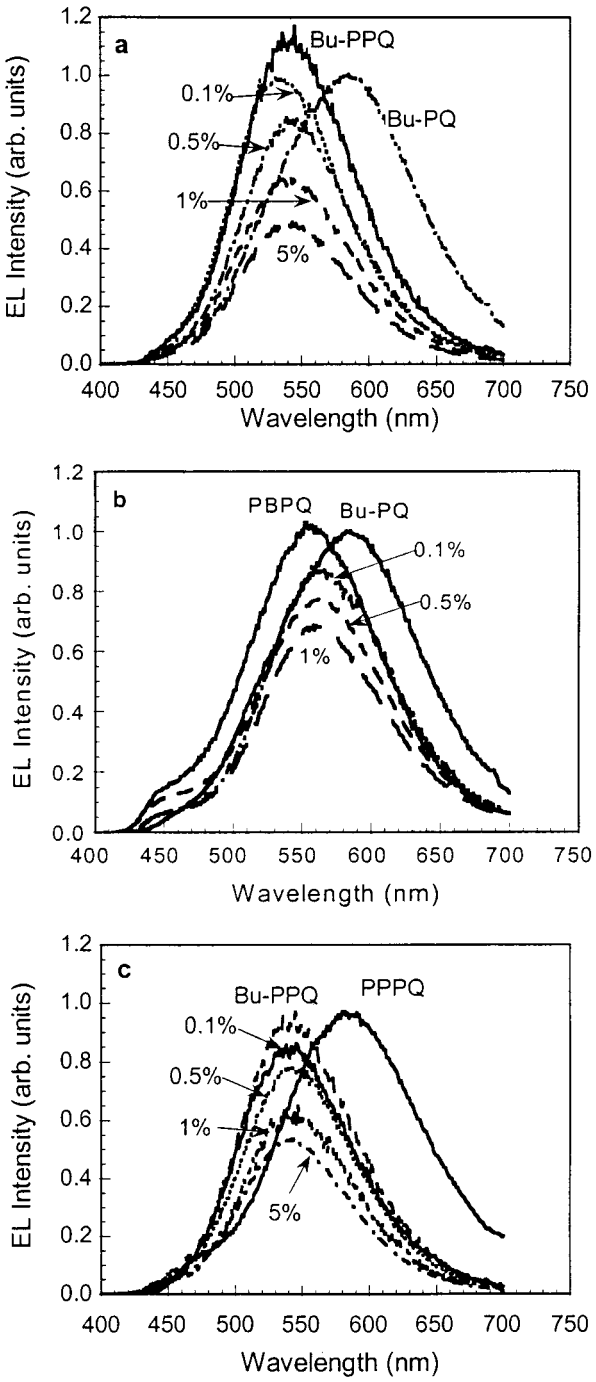

Figure 11. EL spectra of Bu-PQ:Bu-PPQ (a), Bu-PQ:PBPQ (b), and PPPQ:Bu-PPQ (c) blend systems.

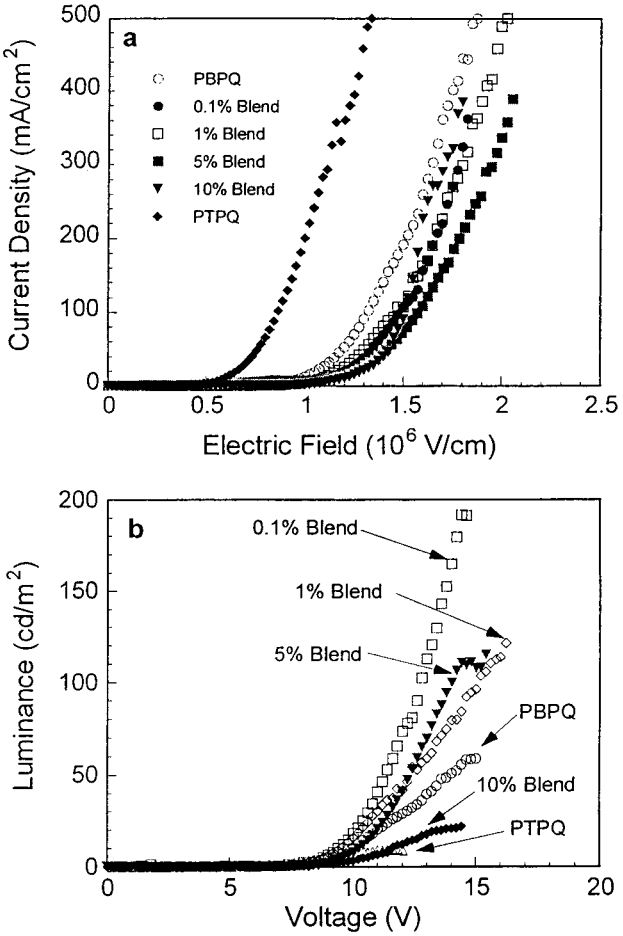

Figure 12. (a) Current density−electric field characteristics of EL devices: PTPQ, PBPQ, 0.1% blend, 1% blend, 5% blend, and 10% blend. (b) Luminance−voltage characteristics of the EL devices in (a).

PBPQ device at the same applied bias voltage. This suggests that the electron−hole recombination efficiency is higher in the blends than in the PBPQ homopolymer, if we assume that the same amounts of charges were injected into the PBPQ and the blends.

The EL quantum efficiency (photons/electron) and luminance of LEDs made from binary blends, compared to devices made from the homopolymers, were dramatically enhanced in the PTPQ:PBPQ and Bu-PQ:PBPQ blends but not enhanced at all in the other two-blend systems (Bu-PQ:Bu-PPQ and PPPQ:Bu-PPQ). Figure 12b shows the luminance−voltage characteristics of the LEDs whose $I-V$ curves are shown in Figure 12a. The PTPQ homopolymer device has a luminance of 10 cd/m^2 at ∼12 V (500 mA/cm^2), the PBPQ device shows a luminance of 50 cd/m^2 at 14 V (400 mA/cm^2), and the 1% and 0.1% blends show luminance of ∼90 and ∼200 cd/m^2 (250 mA/cm^2), respectively, at 14 V. Therefore, the 0.1% blend device shows 4 times enhancement in terms of device brightness compared to the PBPQ device and 20 times enhancement compared to the PTPQ device.

As pointed out above, the current passing through the blend LEDs is smaller than that passing through the devices from the homopolymers, indicating that there is much more enhancement in the EL efficiency. The estimated EL efficiencies for the devices made from PTPQ, PBPQ, and PTPQ:PBPQ blends are shown in Figure 13. PBPQ and PTPQ show EL efficiencies of 0.15% and 0.016% photons/electron, respectively. The 0.1% PTPQ:PBPQ blend has an EL efficiency of 0.46%. The blends showed 3−30 times enhancement in EL efficiencies compared to those of the homopolymers. The EL efficiencies decrease with increasing concentration of the blends. Similar EL enhancements in the Bu-PQ:PBPQ blend LEDs were about factors of 2−4 times compared to those of the homopolymers (Figure 14a). The LEDs made from Bu-PQ and PBPQ had luminance levels of ∼100 and ∼60 cd/m^2, respectively. The 1% Bu-PQ:PBPQ blend had a luminance of about 200 cd/m^2, whereas the 0.5% and 1% blends had luminance of about 170 cd/m^2. However, no EL performance enhancement was observed in the other two blends investigated, Bu-PQ:Bu-PPQ and PPPQ:Bu-PPQ. As shown in Figure

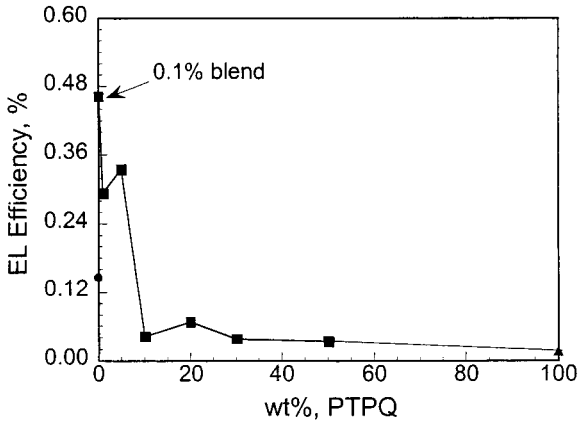

Figure 13. EL efficiency as a function of composition of PTPQ:PBPQ blends: ●, PBPQ; ■, blends; ▲, PTPQ.

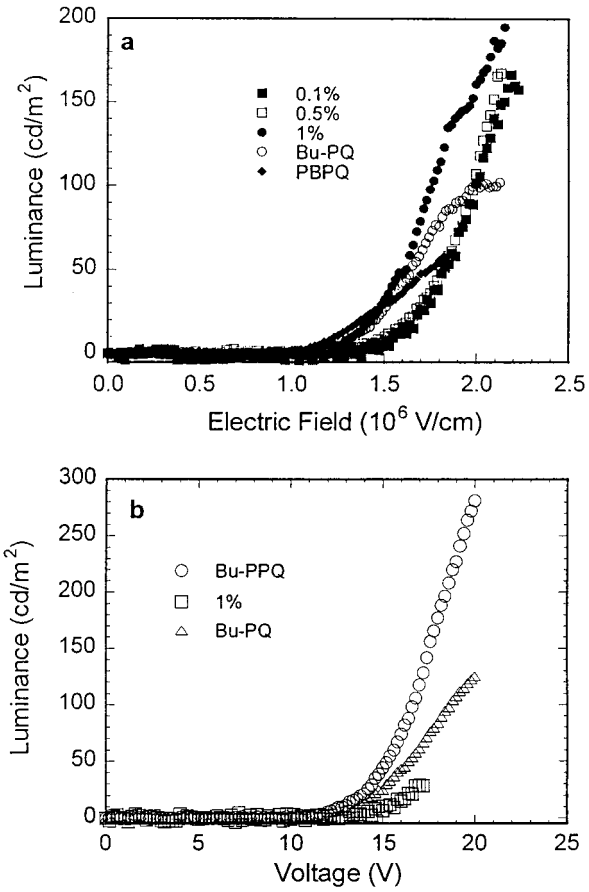

Figure 14. Luminance−voltage (electric field) characteristics of (a) Bu-PQ:PBPQ and (b) Bu-PQ:Bu-PPQ blend systems.

14b, the 1% Bu-PQ:Bu-PPQ had even lower luminance than the homopolymers.

Origin of EL Enhancement in Polymer Blends. In previous reports, the origin of EL enhancement in polymer blends has been attributed to the improved charge carrier injection and transport[7a] and Förster-type (dipole−dipole interactions) energy transfer from the higher excitation energy polymer to the lower energy polymer.[7b,c] EL enhancement in the blends of conjugated polyquinolines reported here cannot be explained by these prior suggestions. In all blends reported here, energy transfer is negligible as discussed above. In fact, we can also clearly rule out improved carrier injection and charge transport as possible factors in the observed EL enhancement. This is because of the similarity of the $I-V$ characteristics and turn-on voltages of the blends compared to those of the host or majority component in the polymer blends discussed above. Furthermore, similar charge injection and transport was operational in the two-blend systems (Bu-PQ:Bu-PPQ and PPPQ:Bu-PPQ) where no EL enhancement was observed. We propose that the observed EL enhancement in binary blends of polyquinolines arises primarily from the spatial confinement of excitons in the dispersed (minority) component.

From both optical absorption and electrochemistry we determined the HOMO/LUMO energy levels of PTPQ and PBPQ which are illustrated in Figure 4a. It can be seen that excitons can be energetically confined within PTPQ molecules in a blend. This can lead to improved electron−hole recombination efficiency. Such a spatial confinement of excitons also leads to improved exciton stability and longer excited state lifetime, which means that the excitons have a higher probability to decay radiatively or nonradiatively. Spatial confinement of excitons achieved with dilute blends (<10%) ensured improved radiative recombination and exciton stability in the two-blend systems, PTPQ:PBPQ and Bu-PQ:PBPQ in which EL enhancement was observed. Figures 12b and 13 clearly show that large EL enhancement was only observed in blends with concentrations less than 10%. This is a result of changes of the local morphology of the blends with varying composition. The composition-dependent morphology of PTPQ:PBPQ blends was previously discussed in connection with the time-resolved PL decay results. We believe that the previously reported large EL enhancement in polymer blends, which was always observed in the low concentration range of the lower energy polymer,[7b,c] as well as some doped organic small molecule LEDs,[22] can now also be understood at least partly in terms of spatial confinement effects.

Improved electron−hole recombination efficiency in the blends was concluded from the current−voltage characteristics of the devices. Figure 12a clearly shows that the 1% and 0.1% blend LEDs have lower current than the devices of the homopolymers. For example, at 14 V (1.75 MV/cm), the PBPQ device showed a current density of 400 mA/cm^2, whereas the two-blend LEDs had a current density of only 250 mA/cm^2. All the three devices have the same emission layer thickness of 30 nm and hole-transport layer thickness of 50 nm. Similarly, the charge injection properties of the three devices are the same since they all showed the same turn-on voltage.

Spatial confinement-induced exciton stability was explored by applying the electric-field-modulated photoluminescence spectroscopy. Electric-field-induced PL quenching in conjugated homopolymers which is caused by exciton dissociation is well-known.[9b,23] Our group has previously observed remarkably high exciton stability under high electric fields when the excitons were confined in semiconducting quantum wire structures consisting of block copolymer/homopolymer blends.[9b] The PL spectra of PTPQ, 0.1% blend, and 10% blend devices under various reverse bias voltages are shown in Figure 15. The measurements under forward bias voltages before the EL device turned on gave identical PL spectra as those under reverse bias voltages, indicating that only the electric field affects the PL spectra and that there is no contribution from EL emission. To obtain PL spectra under higher electric fields, we

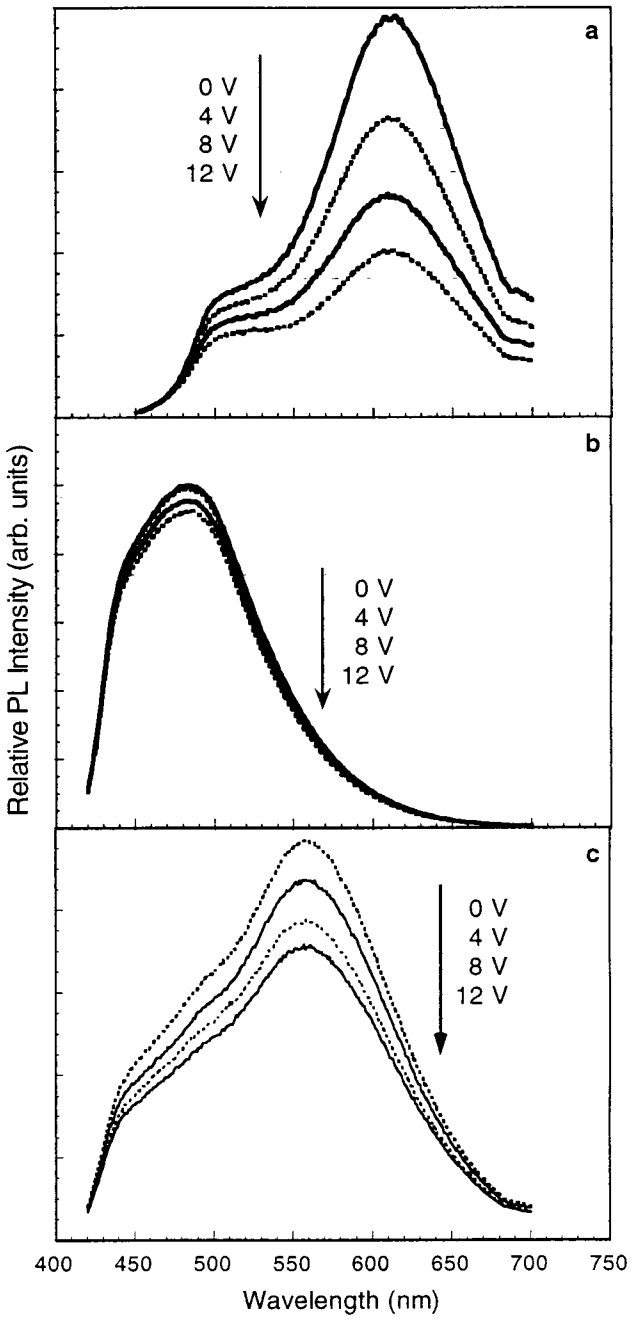

Figure 15. Electric-field-modulated PL spectra of (a) PTPQ, (b) 0.1% blend, and (c) 10% blend at various reverse bias voltages. Blends were excited at 400 nm, and PTPQ was excited at 430 nm.

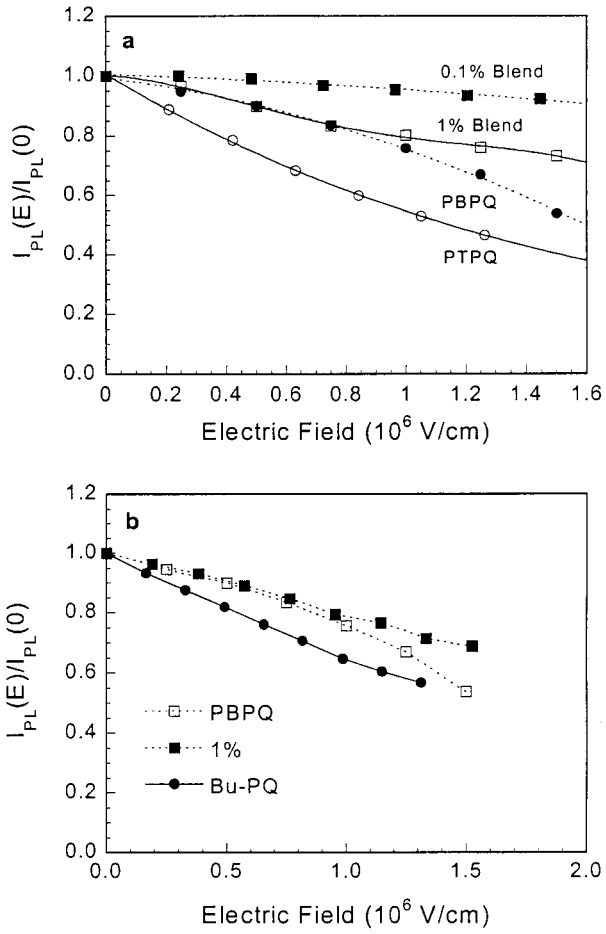

Figure 16. PL quenching as a function of electric field: (a) PTPQ, PBPQ, 0.1% and 1% PTPQ:PBPQ blend; (b) Bu-PQ, PBPQ, and 1% Bu-PQ:PBPQ blend. (Bu-PQ, PBPQ, and all blends were excited at 400 nm, and PTPQ was excited at 430 nm.)

applied reverse bias voltages where there is no EL emission. Figure 15a shows that the PL intensity of the PTPQ device drops about 50% from 0 to 12 V. On the other hand, the 0.1% blend shows less than 10% PL quenching (Figure 15b). The 10% blend showed about 30% of PL quenching (Figure 15c).

Figure 16 shows the relative PL efficiency for blends and the homopolymers as a function of electric field. $I_{PL}(0)$ stands for the integrated PL intensity without electric field and $I_{PL}(E)$ standing for the integrated PL intensity under electric field. PTPQ and PBPQ show 60% and 50% quenching at the highest electric field ($\sim 1.5 \times 10^6$ V/cm) (Figure 16a). The 0.1% and 1% blends show only 10% and 25% quenching, respectively. Figure 16b shows the relative PL efficiency for the 1% Bu-PQ:PBPQ blend and the corresponding homopolymers as a function of electric field. Both Bu-PQ and PBPQ show about 50% PL quenching at the electric field of 1.5×10^6 V/cm, which is a typical operational electric field of polymer LEDs. However, the 1% blend showed only 30% quenching at the same field. This clearly reveals the spatial confinement induced exciton stability in blends of PTPQ:PBPQ and Bu-PQ:PBPQ, which means that exciton dissociation into free charge carriers is much more difficult in polymer blends. Thus, the probability for excitons to decay radiatively was increased and hence the observed EL enhancement in these blends.

Conclusions

Electroluminescence of binary blends of conjugated polyquinolines was investigated using four different model blend systems of PTPQ:PBPQ, Bu-PQ:PBPQ, Bu-PQ:Bu-PPQ, and PPPQ:Bu-PPQ. A 3−30 times enhancement of EL efficiency and LED brightness of the blends compared to those of the homopolymers was observed. From the estimated HOMO/LUMO energy levels of the component polymers, the current−voltage characteristics of the EL devices, and the results of electric-field-modulated photoluminescence spectroscopy, we conclude that the observed EL enhancement in the blends originates primarily from the spatial confinement of excitons which leads to improved exciton stability and electron−hole recombination efficiency.

These results have implications for designing and developing new supramolecular materials for electronic, optoelectronic, and photonic applications using multicomponent conjugated polymers. We expect that there will be even larger enhancement of the EL of polymer blends if both exciton confinement and excitation energy transfer could be facilitated.

Acknowledgment. This research was supported by the Office of Naval Research and by the U.S. Army Research Laboratory and the U.S. Army Research Office TOPS MURI (Grant DAAD19-01-1-0676).

References and Notes

(1) (a) Paul, D. R., Newman, S., Eds. *Polymer Blends*; Academic Press: Orlando, FL, 1978. (b) Ultracki, L. A. *Polymer Alloys and Blends*; Hanser Publishers: Munich, 1990.
(2) Jenekhe, S. A.; de Paor, L. R.; Chen, X. L.; Tarkka, R. M. *Chem. Mater.* **1996**, *8*, 2401−2402.
(3) Yu, G.; Gao, J.; Hummelen, J. C.; Wudl, F.; Heeger, A. J. *Science* **1995**, *270*, 1789−1791.
(4) Chen, X. L.; Jenekhe, S. A. *Macromolecules* **1997**, *30*, 1728−1733.
(5) (a) Halls, J. J. M.; Walsh, C. A.; Greenham, N. C.; Marseglia, E. A.; Friend, R. H.; Moratti, S. C.; Holmes, A. B. *Nature* **1995**, *376*, 498−500. (b) Zhang, X.; Alanko, A. K.; Jenekhe, S. A. *Proc. SPIE−Int. Soc. Opt. Eng.* **1997**, *3144*, 41−52. (c) Jenekhe, S. A.; Yi, S. *Adv. Mater.* **2000**, *12*, 1274−1278.
(6) Yang, C.-J.; Jenekhe, S. A. *Supramol. Sci.* **1994**, *1*, 91−101.
(7) (a) Nishino, H.; Yu, G.; Heeger, A. J.; Chen, T.-A.; Rieke, R. D. *Synth. Met.* **1995**, *68*, 243−247. (b) Yu, G.; Nishino, H.; Heeger, A. J.; Chen, T.-A.; Rieke, R. D. *Synth. Met.* **1995**, *72*, 249−252. (c) Lee, J.-I.; Kang, I.-N.; Hwang, D.-H.; Shim, H.-K. *Chem. Mater.* **1996**, *8*, 1925−1929. (d) Zhang, X.; Shetty, A. S.; Jenekhe, S. A. *Proc. SPIE−Int. Soc. Opt. Eng.* **1997**, *3148*, 89−101.
(8) Jenekhe, S. A.; de Paor, L. R.; Fischer, G. L.; Boyd, R. W., unpublished results.
(9) (a) Chen, X. L.; Jenekhe, S. A. *Macromolecules* **1996**, *29*, 6189−6192. (b) Chen, X. L.; Jenekhe, S. A. *Appl. Phys. Lett.* **1997**, *70*, 487−489.
(10) Chen, X. L. Ph.D. Thesis, University of Rochester: Rochester, 1999.
(11) Gupta, R.; Stevenson, M.; Dogariu, A.; McGehee, M. D.; Park, J. Y.; Srdanov, V.; Wang, H. *Appl. Phys. Lett.* **1998**, *73*, 3492−3494.
(12) (a) Berggren, M.; Inganas, O.; Gustafsson, G.; Rasmusson, J.; Andersson, M. R.; Hjertberg, T.; Wennerstrom, O. *Nature* **1994**, *372*, 444−446. (b) Granstrom, M.; Inganas, O. *Appl. Phys. Lett.* **1996**, *68*, 147−149. (c) Shim, H. K.; Kang, I. N.; Jang, M. S.; Zyung, T.; Jung, S. D. *Macromolecules* **1997**, *30*, 7749−7752.
(13) (a) Inganas, O.; Berggren, M.; Andersson, M. R.; Gustafsson, G.; Hjertberg, T.; Wennerstrom, O.; Dyreklev, P.; Granstrom, M. *Synth. Met.* **1995**, *71*, 2121−2124. (b) Tasch, S.; List, E. J. W.; Ekstrom, O.; Graupner, W.; Leising, G.; Schlichting, P.; Rohr, U.; Geerts, Y.; Scherf, U.; Mullen, K. *Appl. Phys. Lett.* **1997**, *71*, 2883−2885.
(14) (a) Jenekhe, S. A.; Osaheni, J. A. *Science* **1994**, *265*, 765−768. (b) Osaheni, J. A.; Jenekhe, S. A. *Macromolecules* **1994**, *27*, 739−742. (c) Gebler, D. D.; Wang, Y. Z.; Blatchford, J. W.; Jessen, S. W.; Fu, D. K.; Swager, T. M.; MacDiarmid, A. G.; Epstein, A. J. *Appl. Phys. Lett.* **1997**, *70*, 1644−1646. (d) Alam, M. M.; Jenekhe, S. A. *J. Phys. Chem. B* **2001**, *105*, 2479−2482.
(15) (a) Zhang, X.; Shetty, A. S.; Jenekhe, S. A. *Macromolecules* **2000**, *33*, 2069−2082. (b) Zhang, X.; Shetty, A. S.; Jenekhe, S. A. *Macromolecules* **1999**, *32*, 7422−7429. (c) Jenekhe, S. A.; Zhang, X.; Chen, X. L.; Choong, V. E.; Gao, Y.; Hsieh, B. R. *Chem. Mater.* **1997**, *9*, 409−412. (d) Zhang, X.; Shetty, A. S.; Jenekhe, S. A. *Acta Polym.* **1998**, *49*, 52−55.
(16) (a) Agrawal, A. K.; Jenekhe, S. A. *Chem. Mater.* **1996**, *8*, 579−589. (b) Agrawal, A. K.; Jenekhe, S. A. *Macromolecules* **1993**, *26*, 895−905. (c) Agrawal, A. K.; Jenekhe, S. A. *Chem. Mater.* **1993**, *5*, 633−640. (d) Agrawal, A. K.; Jenekhe, S. A. *Chem. Mater.* **1992**, *4*, 95−104. (e) Agrawal, A. K.; Jenekhe, S. A.; Vanherzeele, H.; Meth, J. S. *J. Phys. Chem.* **1992**, *96*, 2837−2843. (f) Abkowitz, M. A.; Stolka, M.; Antoniadis, H.; Agrawal, A. K.; Jenekhe, S. A. *Solid State Commun.* **1992**, *83*, 937−941.
(17) (a) Borsenberger, P. M.; Magin, E. H.; Fitagerald, J. J. *J. Phys. Chem.* **1993**, *97*, 9213−9216. (b) Jenekhe, S. A.; Johnson, P. O.; Agrawal, A. K. *Macromolecules* **1989**, *22*, 3216−3222. (c) Jenekhe, S. A.; Johnson, P. O. *Macromolecules* **1990**, *23*, 4419−4429.
(18) (a) Osaheni, J. A.; Jenekhe, S. A. *J. Am. Chem. Soc.* **1995**, *117*, 7389−7398. (b) Osaheni, J. A.; Jenekhe, S. A.; Perlstein, J. *Appl. Phys. Lett.* **1994**, *64*, 3112−3114. (c) Osaheni, J. A.; Jenekhe, S. A.; Perlstein, J. *J. Phys. Chem.* **1994**, *98*, 12727−12736. (d) Tarkka, R. M.; Zhang, X.; Jenekhe, S. A. *J. Am. Chem. Soc.* ***1996***, *118*, 9438−9439.
(19) Jenekhe, S. A.; Chen, X. L. *Science* **1998**, *279*, 1903−1907. (b) Jenekhe, S. A.; Chen, X. L. *J. Phys. Chem. B* **2000**, *104*, 6332−6335.
(20) Lin, L.-B.; Young, R. H.; Mason, M. G.; Jenekhe, S. A.; Borsenberger, P. M. *Appl. Phys. Lett.* **1998**, *72*, 864−866.
(21) Cimrova, V.; Neher, D. *J. Appl. Phys.* **1996**, *79*, 3299−3306.
(22) Tang, C. W.; VanSlyke, S. A.; Chen, C. H. *J. Appl. Phys.* **1989**, *65*, 3610−3616.
(23) Deussen, M.; Scheidler, M.; Bassler, H. *Synth. Met.* **1995**, *73*, 123−129.

MA0112164